

Correlation between torsional vibration and translational vibration

V. Jeng[†] and Y. L. Tsai[‡]

National Taiwan University of Science and Technology, 43 Keelung Rd. Sec. 4,
Taipei, Taiwan, P. O. BOX 90-130, R.O.C.

(Received September 22, 2001, Accepted March 19, 2002)

Abstract. This paper presents theoretical investigation on the cross correlation between torsional vibration (u_θ) and translation vibration (u_x) of asymmetrical structure under white noise excitation. The formula reveals that the cross correlation coefficient (ρ) is a function of uncoupled frequency ratio ($\Omega = \omega_\theta/\omega_x$), eccentricity, and damping ratio (ξ). Simulations involving acceleration records from fifteen different earthquakes show correlation coefficients results similar to the theoretical correlation coefficients. The uncoupled frequency ratio is the dominating parameter to ρ ; generally, ρ is positive for $\omega_\theta/\omega_x > 1.0$, negative for $\omega_\theta/\omega_x < 1.0$, and close to zero for $\omega_\theta/\omega_x = 1.0$. When the eccentricity or damping ratio increases, ρ increases moderately for small Ω (< 1.0) only. The relation among u_x , u_θ and corner displacement are best presented by ρ ; a simple way to hand-calculate the theoretical dynamic corner displacements from u_x , u_θ and ρ is proposed as an alternative to dynamic analysis.

Key words: dynamic; torsion; seismic response; effective eccentricity; cross correlation; static design; design eccentricity; white noise.

1. Introduction

During an earthquake, asymmetrical structures experience both torsional vibration (u_θ) and lateral vibration (u_x). When these two vibrations combine, they can cause extensive deformation and damage to corner columns; during the 1985 Mexico City Earthquake, torsional vibration was reported as the major cause of damage in 42% of the collapsed or severely damaged buildings (Rosenblueth and Meli 1986). Accordingly, most building codes incorporate special torsional provisions, requiring the design to apply the story shear to the locations around the center of mass (CM). One approach for approximating the equivalent static design involving the concept of effective eccentricity such that the corner displacement is matched with the corresponding quantity calculated in a dynamic analysis (Chandler and Hutchinson 1988, Rutenberg and Pekau 1987). Figs. 2(a) and 2(b) illustrate the effective eccentricities e_f and e_r and the relative peak corner displacements. However, torsional vibration remains as the major concern of the engineering society; and more improvements on the static design procedures are needed for reducing the torsional related damage in the future earthquakes.

[†] Associate Professor

[‡] Ph.D. Candidate

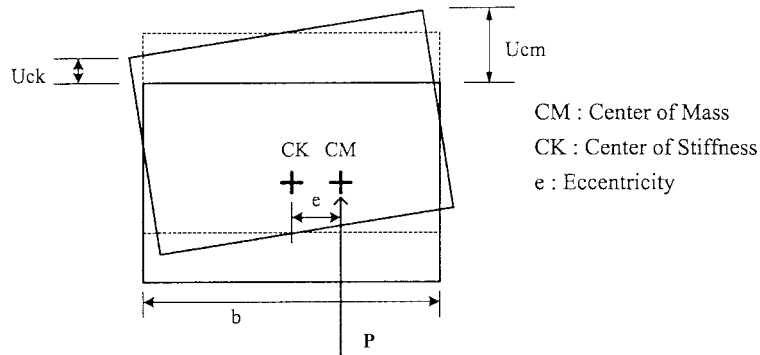


Fig. 1 Corner displacement of structure under static loading

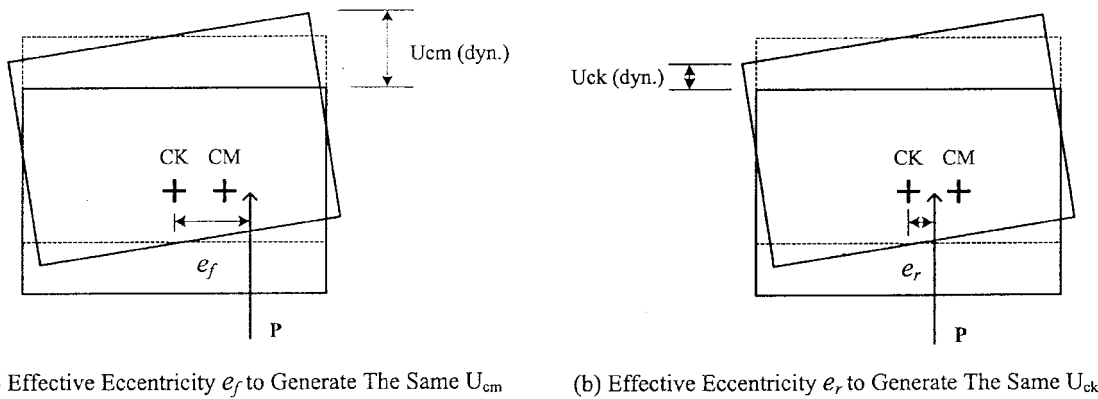


Fig. 2 Corner displacement of structure with effective eccentricity under static loading

Spectral analysis with modal superposition has long been used in dynamic analysis of torsional coupled structure to elucidate the essential effects of eccentricity and uncoupled frequency ratio (ω_θ/ω_x) on the translational and torsional displacements (Kan and Chopra 1976 & 1979, Pan and Kelly 1983, Tso and Dempsey 1980); Interaction equations of the estimated peak responses (e.g., u_x , u_y , and u_θ or base shear and torque) were proposed (Kan and Chopra 1976, Tso and Dempsey 1980) and an upper bound approach assuming peak lateral and torsional displacement occur simultaneously was adopted for estimating the maximum column deformation for elastic system (Kan and Chopra 1979). Meanwhile, the important cross correlation coefficient between u_x and u_θ remains undiscovered for decades.

This investigation applies random vibration theorem and white noise excitation on an ideal two-degree-of-freedom torsionally coupled model to formulate the theoretical correlation coefficient ρ of u_x and u_θ . ρ is found to be a function of uncoupled frequency ratio ($\Omega = \omega_\theta/\omega_x$), eccentricity, and damping ratio. The effects of parameters are investigated and also verified successfully by numerical simulations with acceleration inputs from fifteen different earthquakes. The coefficient is found to be stable for structures with a wide range of natural periods. In general, the white noise excitation assumption facilitates the establishment of the theoretical formula for correlation coefficient and brings the insight into the relations among torsional vibration, translational vibration, and corner displacements.

2. System studied

A one-story structure with a rigid diaphragm, illustrated in Fig. 3, is selected as the ideal model for torsional analysis. The center of stiffness (CK) is at the geometry center of the floor, while the center of mass (CM) is taken to be the center of coordinates. Eccentricity existed on the Y-direction ($e = e_y$) only, but not on the X-direction ($e_x = 0$). Consequently, the lateral displacement u_x in X-direction will be coupled with torsional displacement u_θ when the earthquake ground motion is applied on X-direction. Meanwhile, the mathematical model will neglect vibration on Y-direction, treating it as zero. Therefore, the structure is modeled as a two degrees-of-freedom system. The model is commonly referred as the mass eccentricity system (MES). The assembled lateral stiffness and torsional stiffness at CK are defined as K_x and K_θ , respectively, where $K_\theta = K_x r^2$ and r denotes the radius of gyration of the stiffness around the vertical axis through the stiffness center. The assembled lateral mass and torsional mass at CM are defined as m and m_θ , respectively. Meanwhile, the frequencies (ω_x and ω_θ) of the uncoupled system ($e = 0$) are defined as below:

$$\omega_x = \sqrt{\frac{K_x}{m}} \text{ and } \omega_\theta = \sqrt{\frac{K_\theta}{m_\theta}} \tag{1}$$

where ω_x and ω_θ are the translational and torsional natural frequencies of the uncoupled system, respectively; the uncoupled frequency ratio Ω is defined as

$$\Omega = \frac{\omega_\theta}{\omega_x} \tag{2}$$

The corner displacements (u_{cm} and u_{ck}) can be represented by u_x and u_θ as follow:

$$u_{cm}(t) = u_x(t) + u_\theta(t)(0.5b - e_y)/r = u_x(t) + u_{R1}(t) \tag{3}$$

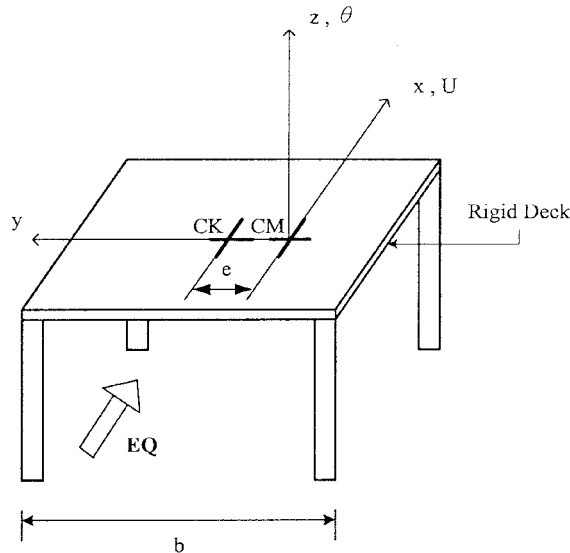


Fig. 3 One story structure model

$$u_{ck}(t) = u_x(t) - u_\theta(t)(0.5b + e_y)/r = u_x(t) - u_{R2}(t) \quad (4)$$

where $u_\theta(t) = r\theta(t)$ and $\theta(t)$ is the angular displacement at CM; $u_{R1}(t)$ and $u_{R2}(t)$ denote the contributions of $\theta(t)$ to the corner displacements; and b represents the dimension of the structure in Y-direction. Hereafter, u_x , u_θ , u_{cm} , u_{ck} , u_{R1} and u_{R2} will be defined as the peak values of $u_x(t)$, $u_\theta(t)$, $u_{cm}(t)$, $u_{ck}(t)$, $u_{R1}(t)$ and $u_{R2}(t)$. From random vibration theory and Eqs. (3) and (4), u_{cm} and u_{ck} could be presented as follows:

$$u_{cm}^2 = u_x^2 + u_{R1}^2 + 2\rho u_x u_{R1} \quad (5)$$

$$u_{ck}^2 = u_x^2 + u_{R2}^2 - 2\rho u_x u_{R2} \quad (6)$$

where ρ is the cross correlation factor of u_x and u_θ . ρ is formulated in the next section based on the random vibration theory with white noise earthquake excitation as input. The peak displacements, u_x , u_θ , u_{cm} and u_{ck} , are obtained either from the random vibration theory by following the process in Der Kiureghian (1981) or just from the modal combination.

3. Mathematical formulation

3.1 Equation of motion

The governing equation of motion of the torsional coupled system under ground excitation in X-direction is presented as follows:

$$\begin{bmatrix} m & 0 \\ 0 & m\frac{r^2}{\Omega^2} \end{bmatrix} \begin{Bmatrix} \ddot{u}_x(t) \\ \ddot{\theta}(t) \end{Bmatrix} + [C] \begin{Bmatrix} \dot{u}_x(t) \\ \dot{\theta}(t) \end{Bmatrix} + \begin{bmatrix} K_x & -K_x e_y \\ -K_x e_y & K_x r^2 \end{bmatrix} \begin{Bmatrix} u_x(t) \\ \theta(t) \end{Bmatrix} = - \begin{bmatrix} m & 0 \\ 0 & m\frac{r^2}{\Omega^2} \end{bmatrix} \{r\} \ddot{u}_{gx}(t) \quad (7)$$

where $[C]$ is the damping matrix, $\{r\} = \{1, 0\}^T$ denotes the influence coefficient vector, and $\ddot{u}_{gx}(t)$ represents the ground acceleration in the X-direction. By defining u_θ as $u_\theta = r\theta$ and conducting eigenvector analysis, the responses could be represented by modal responses y_1 and y_2 .

$$\begin{Bmatrix} u_x(t) \\ u_\theta(t) \end{Bmatrix} = [\Phi] \begin{Bmatrix} y_1(t) \\ y_2(t) \end{Bmatrix} \quad (8)$$

The equations could then be decoupled and the two new independent modal equations are:

$$\ddot{y}_i(t) + 2\xi_i \omega_i \dot{y}_i(t) + \omega_i^2 y_i(t) = -L_i \ddot{u}_{gx}(t), \quad i = 1, 2 \quad (9)$$

where ξ_i is the modal damping ratio, ω_i represents the modal natural frequency, and L_i denotes the

modal participation factor in the i^{th} mode of the system.

The natural frequencies of the system are expressed as

$$\omega_1^2 = \frac{\omega_x^2}{2} \left[1 + \frac{\omega_\theta^2}{\omega_x^2} - \sqrt{\left[\frac{\omega_\theta^2}{\omega_x^2} - 1 \right]^2 + 4 \left[\frac{e_y^2}{r^2} \left(\frac{\omega_\theta}{\omega_x} \right)^2 \right]} \right] \quad (10)$$

$$\omega_2^2 = \frac{\omega_x^2}{2} \left[1 + \frac{\omega_\theta^2}{\omega_x^2} + \sqrt{\left[\frac{\omega_\theta^2}{\omega_x^2} - 1 \right]^2 + 4 \left[\frac{e_y^2}{r^2} \left(\frac{\omega_\theta}{\omega_x} \right)^2 \right]} \right] \quad (11)$$

The related mode shape is given by

$$[\Phi] = [\{\phi^1\} \{\phi^2\}] \quad (12)$$

and

$$\{\phi^i\} = \begin{Bmatrix} \phi_x^i \\ \phi_\theta^i \end{Bmatrix} = \begin{Bmatrix} \frac{\frac{e_y \omega_\theta}{r \omega_x}}{\sqrt{\left(\frac{e_y \omega_\theta}{r \omega_x} \right)^2 + \left(1 - \frac{\omega_i^2}{\omega_x^2} \right)^2}} \\ \left(1 - \frac{\omega_i^2}{\omega_x^2} \right) \frac{\omega_\theta}{\omega_x} \\ \frac{\frac{e_y \omega_\theta}{r \omega_x}}{\sqrt{\left(\frac{e_y \omega_\theta}{r \omega_x} \right)^2 + \left(1 - \frac{\omega_i^2}{\omega_x^2} \right)^2}} \end{Bmatrix} \quad i = 1, 2 \quad (13)$$

Thus, the modal participation factors L_i are

$$L_i = \frac{\left(\frac{e_y}{r} \right) \left(\frac{\omega_\theta}{\omega_x} \right)}{\sqrt{\left(\frac{e_y \omega_\theta}{r \omega_x} \right)^2 + \left(1 - \frac{\omega_i^2}{\omega_x^2} \right)^2}} \quad i = 1, 2 \quad (14)$$

3.2 Formulation of ρ

As commonly assumed in random vibration analysis, the earthquake ground acceleration is considered as white noise. The correlation coefficient ρ of u_x and u_θ is then defined as

$$\rho = \frac{E[u_x(t)u_\theta(t)]}{\sqrt{E[u_x^2(t)]}\sqrt{E[u_\theta^2(t)]}} \quad (15)$$

Meanwhile, the translational and torsional displacements are reconstructed from the modal response as follows:

$$u_x(t) = \phi_x^1 L_1 q_1(t) + \phi_x^2 L_2 q_2(t) \quad (16)$$

$$u_\theta(t) = \phi_\theta^1 L_1 q_1(t) + \phi_\theta^2 L_2 q_2(t) \quad (17)$$

The second moment of $u_x(t)$ is then expressed as follow:

$$E[u_x^2(t)] = (\phi_x^1 L_1)^2 E[q_1^2(t)] + (\phi_x^2 L_2)^2 E[q_2^2(t)] + 2(\phi_x^1 L_1)(\phi_x^2 L_2) E[q_1(t)q_2(t)] \quad (18)$$

where $q_1(t)$, $q_2(t)$ denote spectral response of each mode subjected to white noise excitation, respectively; q_1 and q_2 are the peak value of $q_1(t)$ and $q_2(t)$, respectively. Assume the peak factor K_ρ , the ratio of the maximum displacement and standard deviation of a random process, remain constant as commonly assumed in random vibration theory. The upper equation is then expressed as follows:

$$\begin{aligned} E[u_x^2(t)] &= \frac{1}{K_\rho^2} [(\phi_x^1 L_1)^2 q_1^2 + (\phi_x^2 L_2)^2 q_2^2 + 2\rho_{12}(\phi_x^1 L_1)(\phi_x^2 L_2)q_1 q_2] \\ &= \frac{q_2^2}{K_\rho^2} [(\phi_x^1 L_1)^2 r_q^2 + (\phi_x^2 L_2)^2 + 2\rho_{12} r_q (\phi_x^1 L_1)(\phi_x^2 L_2)] \end{aligned} \quad (19)$$

where $r_q = q_1/q_2$, and ρ_{12} is the correlation between mode 1 and mode 2.

By following the same process used in Eq. (19), the following related equations are obtained.

$$E[u_\theta^2(t)] = \frac{q_2^2}{K_\rho^2} [(\phi_\theta^1 L_1)^2 r_q^2 + (\phi_\theta^2 L_2)^2 + 2\rho_{12} r_q (\phi_\theta^1 L_1)(\phi_\theta^2 L_2)] \quad (20)$$

$$\begin{aligned} E[u_x(t)u_\theta(t)] &= \frac{q_2^2}{K_\rho^2} \{(\phi_x^1 L_1)(\phi_\theta^1 L_1) r_q^2 + (\phi_x^2 L_2)(\phi_\theta^2 L_2) \\ &\quad + \rho_{12} r_q [(\phi_x^1 L_1)(\phi_\theta^2 L_2) + (\phi_x^2 L_2)(\phi_\theta^1 L_1)]\} \end{aligned} \quad (21)$$

The power spectral density of the white noise excitation is a constant G_0 , and the spectral moment of $q_i(t)$ is as follow:

$$E[q_i^2(t)] = \pi G_0 / (4\xi\omega_i^3) \quad (22)$$

Therefore

$$r_q = q_1/q_2 = \{E[q_1^2(t)]/E[q_2^2(t)]\}^{0.5} = (\omega_2/\omega_1)^{1.5} \quad (23)$$

The modal correlation coefficient ρ_{12} of the CQC combination rules (Der Kiureghian 1981) is adopted.

$$\rho_{12}(r_{12}, \xi) = \frac{8\xi^2(1+r_{12})r_{12}^{3/2}}{(1-r_{12}^2)^2 + 4\xi^2r_{12}(1+r_{12})^2} \quad (24)$$

where $r_{12} = \omega_1/\omega_2$, ξ = damping ratio, selected as the same for both modes.

By substituting Eqs. (19)-(22), (24) into Eq. (15), the formula for the correlation coefficient of u_x and u_θ is obtained. However, according to Eqs. (10), (11), (13), (14), (22): ϕ^i , L_i , ω_i/ω_x , ω_1/ω_2 , q_1/q_2 and ρ_{12} are functions of variables e_y/r , ω_θ/ω_x and ξ , by themselves, therefore theoretically the variables of this function could be condensed to only three variables: e_y/r , ω_θ/ω_x and ξ . However, the formula for ρ is too complex to present here, therefore, only the general form is expressed as follows:

$$\rho = f_{CN}\left(\frac{\omega_\theta}{\omega_x}, \xi, \frac{e_y}{r}\right) \quad (25)$$

The second moment of $u_0(t)$ (the translational displacement of uncoupled system ($e = 0$)) can also be expressed the same as Eq. (22):

$$E[u_0^2(t)] = \pi G_0 / (4\xi\omega_x^3) \quad (26)$$

Therefore, the normalized peak displacements, $U = u_x/u_0$; $U_\theta = u_\theta/u_0$, can be obtained from Eqs. (19), (20), (22), (23). The above process can, also obtain the normalized peak corner displacements, U_{cm} , and U_{ck} . All these displacements could also be obtained from modal combinations as an alternative.

4. Theoretical and simulated results

Parameters such as ω_θ/ω_x , ξ , and e/r are investigated according to the theoretical formula for correlation coefficient ρ and the related displacements, U , U_θ , U_{cm} , and U_{ck} .

Numerical simulation is conducted with acceleration input from fifteen different earthquakes, which have been used in author's previous spectral related research (Jeng and Kasai 1996). Parameters such as three different T 's (0.5, 1.0, and 2.0 sec.), four different damping ratios (0.025, 0.05, 0.10, and 0.20), and 11 frequency ratios (ranging from 0.5 to 1.5 with an 0.1 interval) are investigated.

The peak displacements, u_x , u_θ , u_{cm} , and u_{ck} , are obtained from the time history analysis of the torsional coupled system for different periods, frequency ratios, and earthquakes. The peak displacements are then normalized by the peak lateral displacement (u_0) of the uncoupled system to obtain U , U_θ , U_{cm} , and U_{ck} . The correlation coefficient can then be back calculated from Eqs. (5) and (6). All the curves represent the mean of the results of fifteen earthquakes, unless otherwise defined.

4.1 Correlation coefficient ρ

Fig. 4(a) illustrate the ρ curves against the frequency ratio for five different eccentricities ($e/r = 0.025, 0.05, 0.1, 0.2, \text{ and } 0.4$), the ρ curves are close to anti-symmetrical. The curves for smaller eccentricities ($e/r = 0.025, 0.05, 0.1, \text{ and } 0.2$) are almost identical; they start at values around -0.19

at $\omega_\theta/\omega_x = 0.34$, decrease slowly to -0.5 , then rise quickly between $\omega_\theta/\omega_x = 0.8$ and 1.25 , and slowly reach peak at around 1.0 at $\omega_\theta/\omega_x = 3$. The curve for the largest eccentricity ($e/r = 0.4$) is the highest in value than the other curves at $\omega_\theta/\omega_x < 1.0$, and is close to zero. This latter leads to larger u_{cm} as shown in Fig. 5(a). This trend is unmistakable, however, there is no simple explanation. In general, ρ is positive when $\omega_\theta/\omega_x > 1.0$; and ρ is negative when $\omega_\theta/\omega_x < 1.0$. In the random vibration theory, $\rho = 1.0$ represents a complete in-phase between two vibrations; $\rho = -1$ represents a complete out-of-phase; and $\rho = 0$ represents a complete statistical independency between two vibrations. Therefore, a large positive ρ (0.9 at $\omega_\theta/\omega_x = 2$) indicates $u_x(t)$ and $u_\theta(t)$ strongly in-phase and cause the combination to favor a large u_{cm} and a small u_{ck} , according to Eqs. (5) and (6). Meanwhile a negative ρ (-0.5 at $\omega_\theta/\omega_x = 0.8$) indicates $u_x(t)$ and $u_\theta(t)$ strongly out-of-phase and causes the combination to favor a small u_{cm} and a large u_{ck} . Therefore, $\rho = 0$ is the pivot point that separates the cases into three groups: (1) for $\rho > 0$, $u_{cm} > u_{ck}$; (2) for $\rho = 0$, $u_{cm} = u_{ck}$; and (3) for $\rho < 0$, $u_{cm} < u_{ck}$.

Figs. 4(b), 4(c), and 4(d) illustrate the simulated correlation coefficient for three different periods

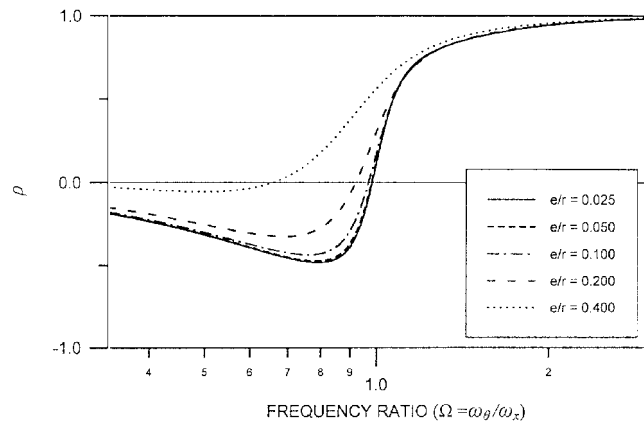


Fig. 4(a) Theoretical correlation coefficient ρ ($\xi = 0.05$, white noise)

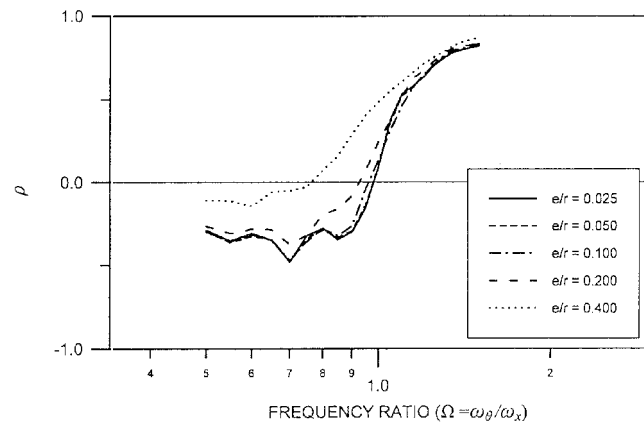


Fig. 4(b) Simulated correlation coefficient ρ ($T = 0.5$ sec., $\xi = 0.05$, results of 15 earthquakes)

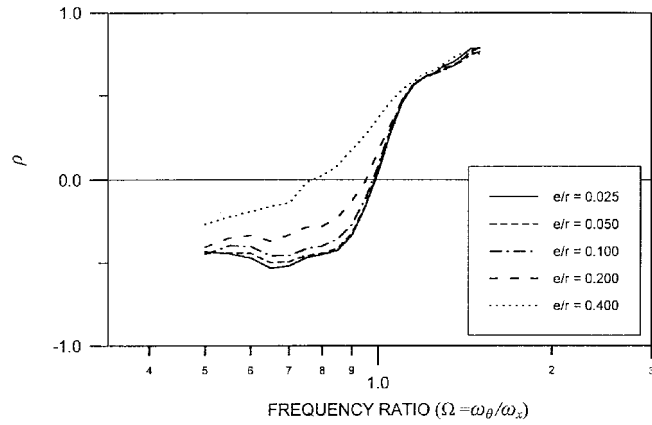


Fig. 4(c) Simulated correlation coefficient ρ ($T = 1.0$ sec., $\xi = 0.05$, results of 15 earthquakes)

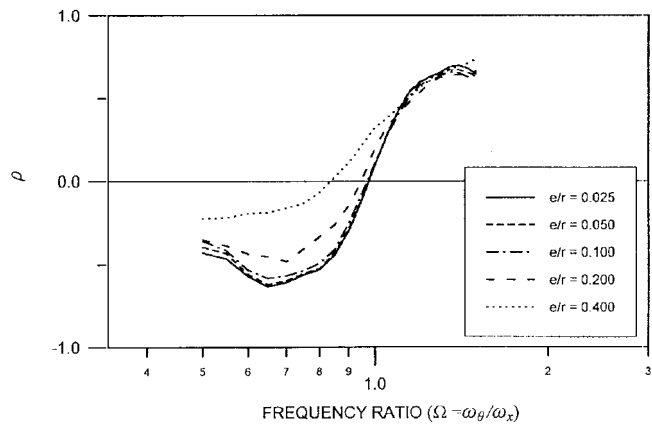


Fig. 4(d) Simulated correlation coefficient ρ ($T = 2.0$ sec., $\xi = 0.05$, results of 15 earthquakes)

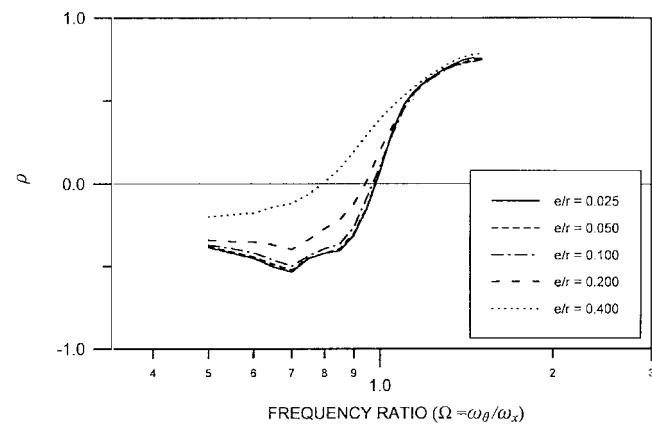


Fig. 4(e) Simulated correlation coefficient ρ (Average results of 3 different periods $T = 0.5, 1.0$ and 2.0 sec., $\xi = 0.05$)

(0.5, 1.0, and 2.0 seconds), respectively; the simulated ρ curves follow the theoretical curves in Fig. 4(a) nicely. However, there exists minor differences; the theoretical results appear to have the highest value, then followed by the results for $T = 0.5$ sec., $T = 1.0$ sec., and $T = 2.0$ sec. This could be caused by the characteristics of the earthquakes applied and need further investigation in the future. But, generally speaking, the resemblance between the theoretical and simulated results is impressive. Fig. 4(e) is the average results for the three different periods.

4.2 Corner displacements

Fig. 5(a) illustrate the theoretical peak corner displacements (U_{cm} and U_{ck}) against the frequency ratios for five different eccentricities ($T = 1.0$ sec., damping ratio 0.05, and $b/r = 2.0$). For $e/r = 0.2$, the maximum value of U_{ck} is 1.4 at $\omega_\theta/\omega_x = 0.75$; and the maximum value of U_{cm} is 1.75 at $\omega_\theta/\omega_x = 1.35$. Generally, U_{ck} curves are above 1.0 and U_{cm} curves below 1.0 when $\omega_\theta/\omega_x < 1.0$; however,

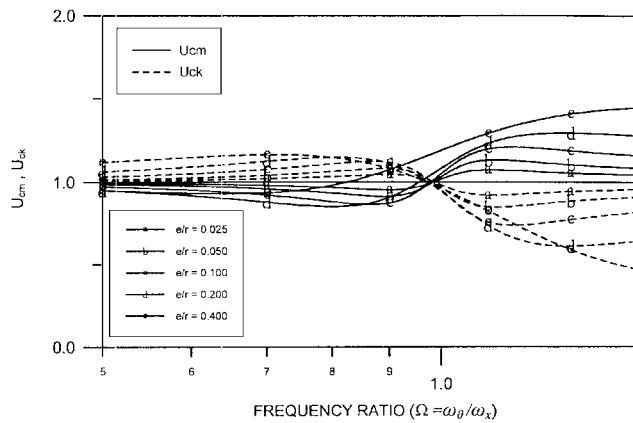


Fig. 5(a) Theoretical normalized corner displacements (U_{cm} , U_{ck}) ($\xi = 0.05$, $b/r = 2$, white noise)

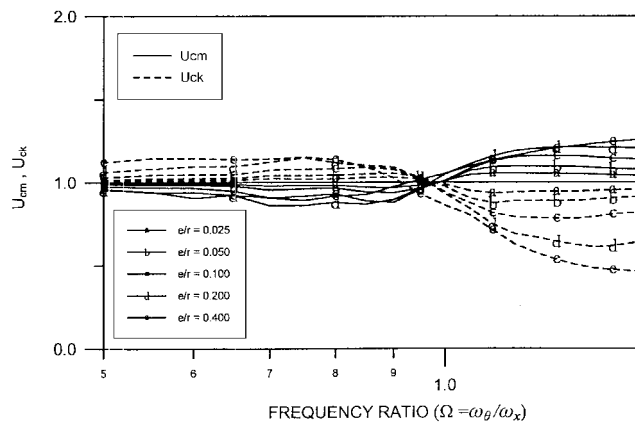


Fig. 5(b) Simulated normalized corner displacements (U_{cm} , U_{ck}) ($T = 0.5$ sec., $\xi = 0.05$, $b/r = 2$, results of 15 earthquakes)

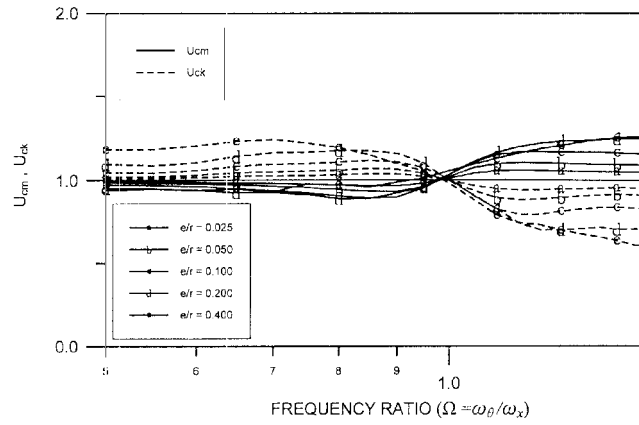


Fig. 5(c) Simulated normalized corner displacements (U_{cm} , U_{ck}) ($T = 1.0$ sec., $\xi = 0.05$, $b/r = 2$, results of 15 earthquakes)

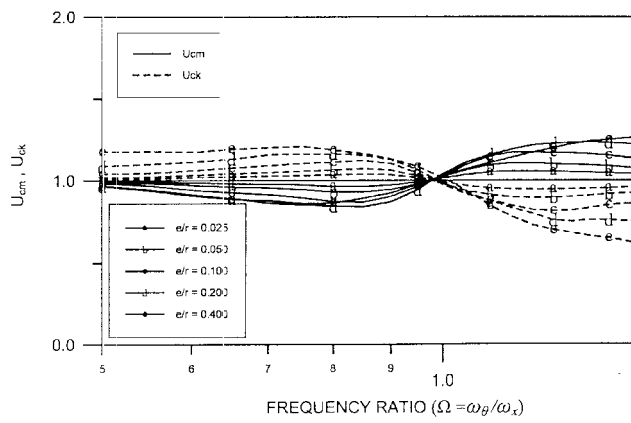


Fig. 5(d) Simulated normalized corner displacements (U_{cm} , U_{ck}) ($T = 2.0$ sec., $\xi = 0.05$, $b/r = 2$, results of 15 earthquakes)

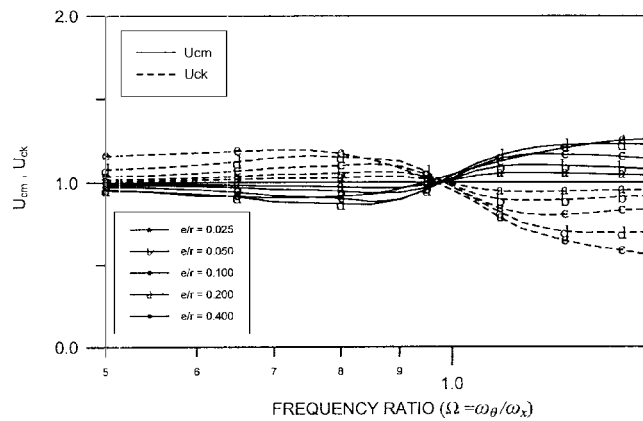


Fig. 5(e) Simulated normalized corner displacements (U_{cm} , U_{ck}) (Average results of 3 different periods $T = 0.5, 1.0$ and 2.0 sec., $\xi = 0.05$, $b/r = 2$)

the relative positions of the curves exchanged when $\omega_\theta/\omega_x > 1.0$. By the other word, U_{cm} and U_{ck} curves follow the trend set by ρ as mentioned in the previous discussion. Figs. 5(b), 5(c), 5(d), and 5(e) display the simulated corner displacements for the cases $T = 0.5$ sec., 1.0 sec., 2.0 sec., and the average. Again, the simulated results have the similar trends as the theoretical results in Fig. 5(a) except with smaller values. This will be discussed later in session 5.

4.3 U , U_θ , and DAF

Figs. 6, 7, and 8 present both the theoretical results and simulated results of U , U_θ , and the Dynamic Amplification Factor (DAF), respectively. Be noticed in Figs. 6 (U curves) for large eccentricity cases ($e/r = 0.4$), the shift of the natural frequencies (see Eqs. (10) and (11)) causes the theoretical curve with higher value for large Ω and not as symmetrical as the curves for small eccentricity. DAF is defined as the dynamic peak u_θ divided by the static u_θ caused by the equivalent

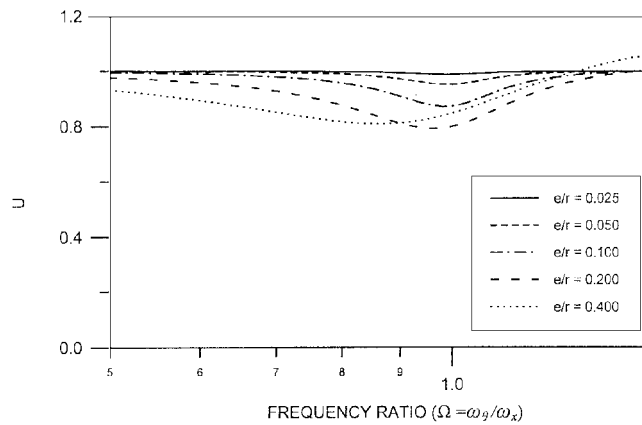


Fig. 6(a) Theoretical normalized lateral displacement U ($\xi = 0.05$, $b/r = 2$, white noise)

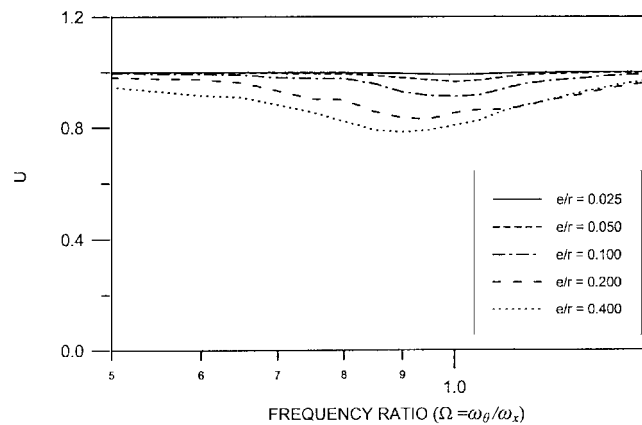


Fig. 6(b) Simulated normalized lateral displacement U ($T = 0.5$ sec., $\xi = 0.05$, $b/r = 2$, results of 15 earthquakes)

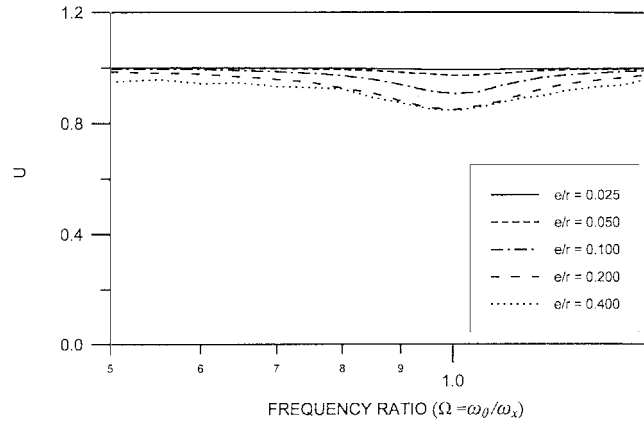


Fig. 6(c) Simulated normalized lateral displacement U ($T = 1.0$ sec., $\xi = 0.05$, $b/r = 2$, results of 15 earthquakes)

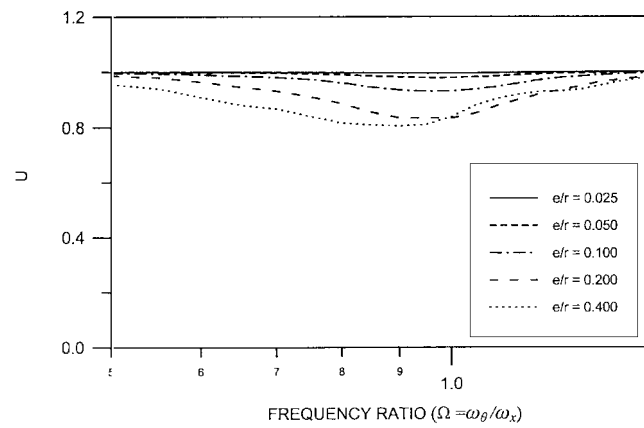


Fig. 6(d) Simulated normalized lateral displacement U ($T = 2.0$ sec., $\xi = 0.05$, $b/r = 2$, results of 15 earthquakes)

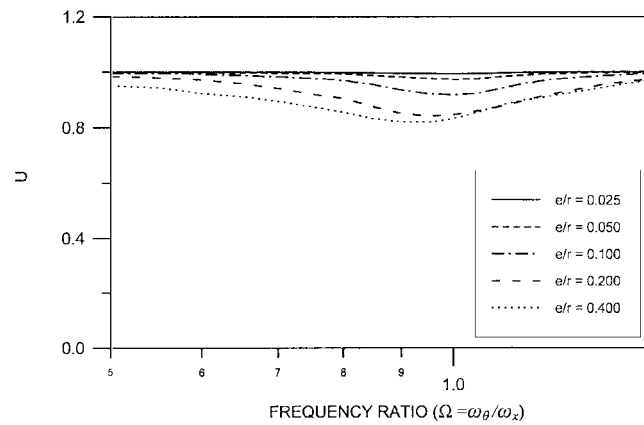


Fig. 6(e) Simulated normalized lateral displacement U (Average results of 3 different periods $T = 0.5$, 1.0 and 2.0 sec., $\xi = 0.05$, $b/r = 2$)

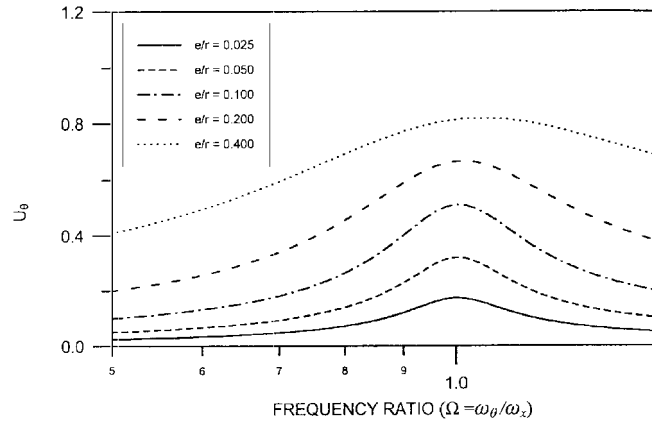


Fig. 7(a) Theoretical normalized torsional displacement U_θ ($\xi = 0.05$, $b/r = 2$, white noise)

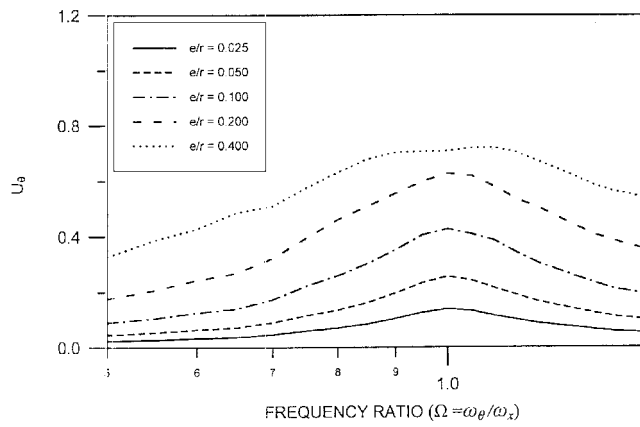


Fig. 7(b) Simulated normalized torsional displacement U_θ ($T = 0.5$ sec., $\xi = 0.05$, $b/r = 2$, results of 15 earthquakes)

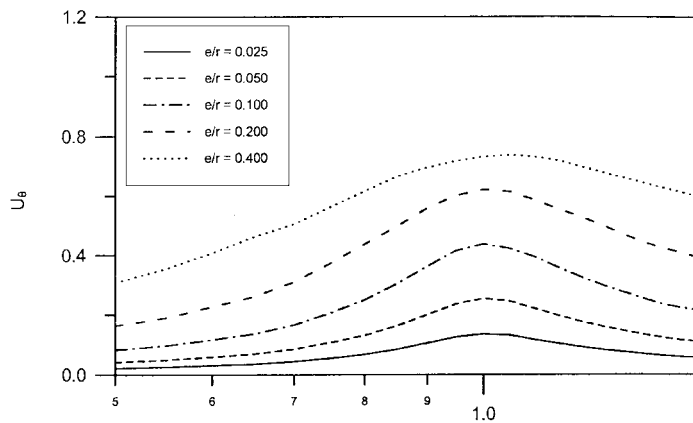


Fig. 7(c) Simulated normalized torsional displacement U_θ ($T = 1.0$ sec., $\xi = 0.05$, $b/r = 2$, results of 15 earthquakes)

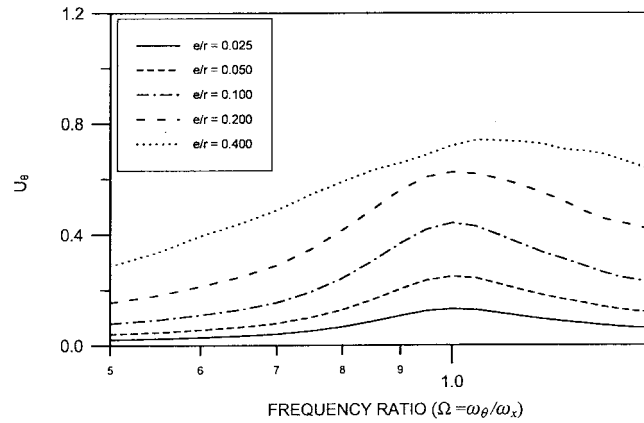


Fig. 7(d) Simulated normalized torsional displacement U_θ ($T = 2.0$ sec., $\xi = 0.05$, $b/r = 2$, results of 15 earthquakes)

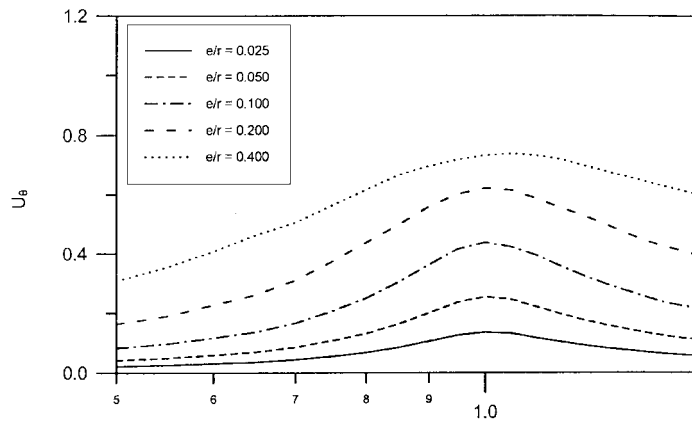


Fig. 7(e) Simulated normalized torsional displacement U_θ (Average results of 3 different periods $T = 0.5$, 1.0 and 2.0 , $\xi = 0.05$, $b/r = 2$)

lateral static force on the CM. Again, the simulation results in Figs. 7 and 8 show slightly smaller values comparing to the theoretical results in Figs. 7(a) and 8(a), respectively.

4.4 Damping ratio

Fig. 9 presents the theoretical ρ curves ($e/r = 0.2$) with four different damping ratios ($\xi = 0.025$, 0.05 , 0.10 , and 0.20) against the frequency ratios. Higher damping ratio influence the shape of the ρ curves in the same manners as higher eccentricity; the curve of higher damping ratio move up at small Ω (<1).

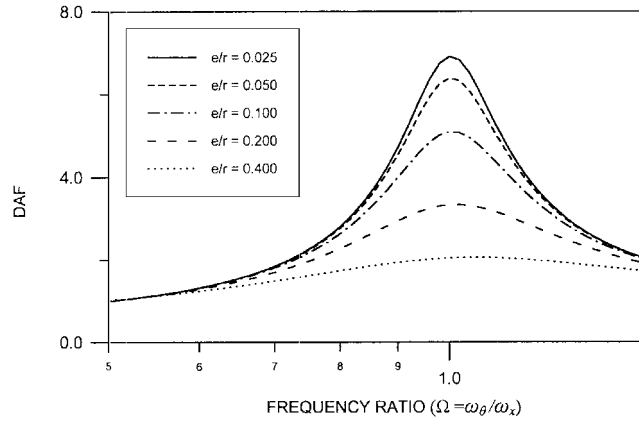


Fig. 8(a) DAF ($\xi = 0.05$, $b/r = 2$, white noise)

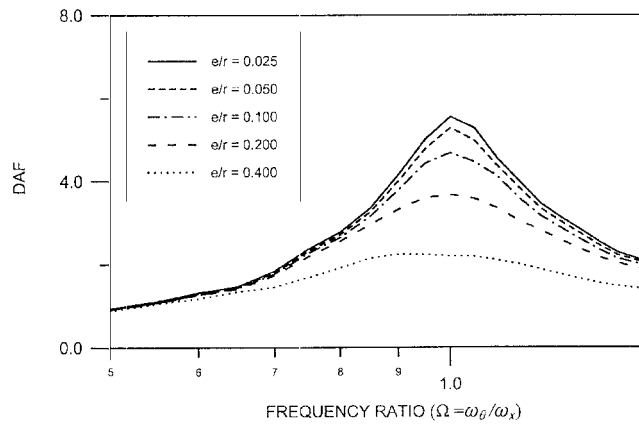


Fig. 8(b) DAF ($T = 0.5$ sec., $\xi = 0.05$, $b/r = 2$, results of 15 earthquakes)

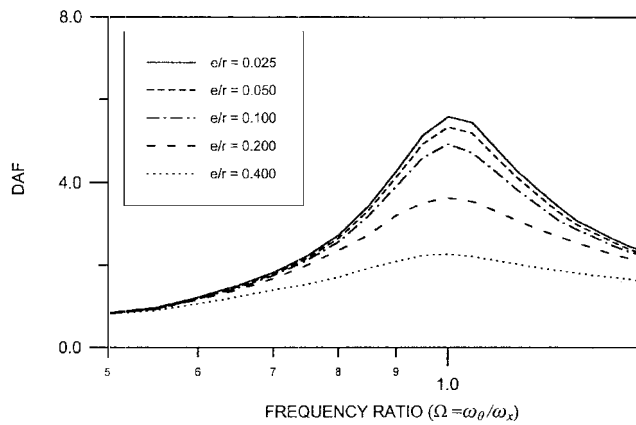


Fig. 8(c) DAF ($T = 1.0$ sec., $\xi = 0.05$, $b/r = 2$, results of 15 earthquakes)

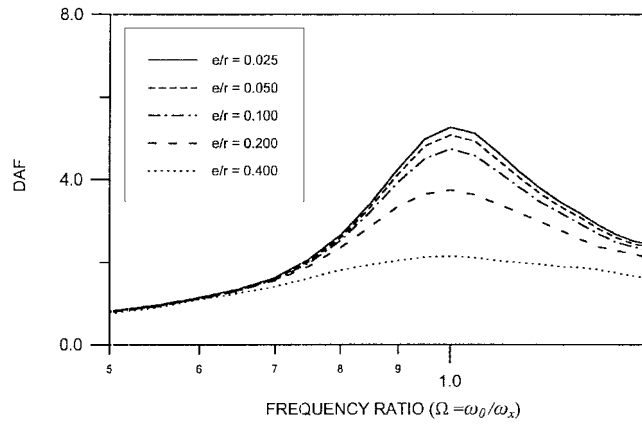


Fig. 8(d) DAF ($T = 2.0$ sec., $\xi = 0.05$, $b/r = 2$, results of 15 earthquakes)

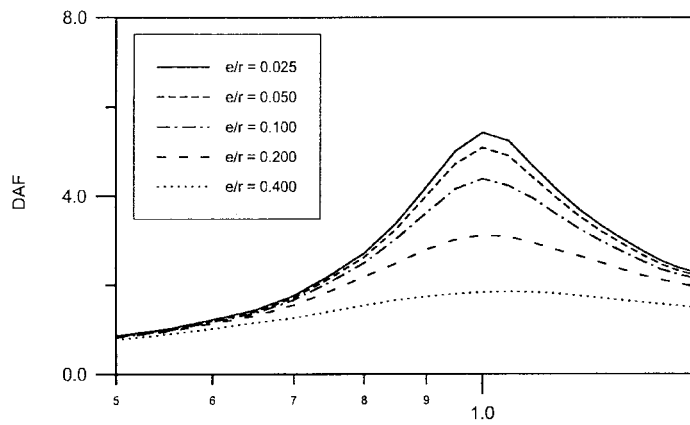


Fig. 8(e) DAF (Average results of 3 different periods $T = 0.5, 1.0$ and 2.0 sec., $\xi = 0.05$, $b/r = 2$)

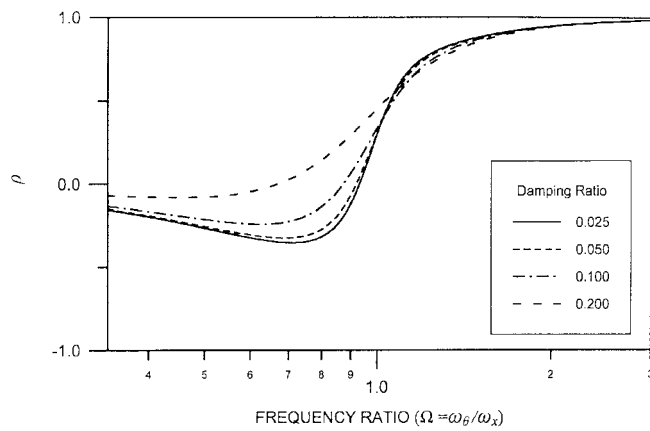


Fig. 9 Theoretical correlation coefficient ρ ($e/r = 0.2$, White noise)

4.5 Comparison to correlation coefficient of modal combination

Generally, the correlation ρ between u_x and u_θ decreases when frequency ratio approaches 1.0 or damping ratio is higher (see Fig. 4(a)). This behavior is in contrast to the correlation coefficient ρ_{12} for modal combinations; ρ_{12} increases when frequency ratio of the two modes approach 1.0 or damping ratio is higher, as demonstrated by Eq. (24).

5. Discussion

5.1 White noise assumption

White noise assumption allow the formula of the correlation be established conveniently, and the correlation coefficient brings insight into the relation between torsional and translational vibration. The theoretical results match the earthquake simulation results nicely. However, the results from simulation tend to have smaller values comparing to the theoretical results, this is become notable for large eccentricity cases ($e/r = 0.4$). Possible reasons might include (1) duration of the real earthquakes is limited comparing to the unlimited duration of white noise excitation, therefore the theoretical model under white noise excitation has higher probability to generate larger vibrations. (2) white noise excitation has different frequency content comparing to earthquakes. In spite of these differences, the average torsional responses of the asymmetrical structure under large number of earthquake excitations are very close to the responses under white noise excitation, therefore the white noise assumption to represent the average earthquake appear as satisfactory.

5.2 Model restriction in torsional analysis

The maximum corner displacements obtained from torsional analysis of the asymmetrical structure adopting different model (MES or SES) are known to be different. Therefore, the building codes adopted research results derived from one of the model (MES or SES) will have difficulty applying to structures with the other model or with arbitrary geometry.

The curves of ρ , U , and U_θ are derived from Eq. (7), which is independent of geometry factors of the structure. For elastic systems, the different structural model (or configuration) could be introduced (after ρ , U , and U_θ are already derived), and the resulted peak corner displacements for different model could then be calculated by introducing proper U_{R1} and U_{R2} into Eqs. (5) and (6) based on the edge distance from CM. Therefore, the difference in modeling is not a problem in elastic analysis, as long as the correlation is recognized as a key parameter; peak corner displacements for any specific model could be generated from ρ , U , and U_θ , accordingly.

Therefore, one major advantage of this new approach over the others is that its results could be easily apply to structures with all kind of geometry (different model, b/r) where the results of other approach are restricted to the model they adopted.

The latter examples (1) and (2) will demonstrate the difference in peak corner displacement and effective eccentricity caused by these two models for structure with the same eccentricity (e), and they could all be derived from the new approach.

5.3 Calculating corner displacement

Although u_x and u_θ were studied with respect to eccentricity and frequency ratio and similar curves were proposed by researchers in the past (Chandler and Hutchinson 1988, Rutenberg and Pekau 1987, Kan and Chopra 1976 & 1979), there was no rules to combine u_x and u_θ into design essential corner displacements. With the proposed correlation coefficient, u_{cm} and u_{ck} can be obtained through Eqs. (5) and (6) as shown in the following Example 1 and 2. This is an attractive alternative to calculate the theoretical dynamic corner displacements without the complex calculation of dynamic analysis.

Example 1. Consider an example structure, as in Fig. 1 (MES), ($e/r = 0.20$, uncouple translational period $T = 1.0$ second, frequency ratio = 1.25, $b/r = 2.0$, and damping ratio 5%) is subjected a white noise type earthquake, and the peak lateral displacement (u_0) for the uncoupled system is known to be 10 cm. The theoretical dynamic peak responses u_x , u_θ , u_{cm} , and u_{ck} can be obtained as follows:

(A) Static corner displacement

Corner displacement is calculated by applying equivalent static force on the CM, this is according to UBC (Uniform Building Code 1997) but with the 5% b accidental eccentricity neglected here.

$$u_{cm} = 10 \times (1 + 0.5(e/r)(b/r)) = 10 (1 + 0.5 \times 0.2 \times 2) = 12 \text{ cm}$$

$$u_{ck} = 10 \times (1 - 0.5(e/r)(b/r)) = 10 (1 - 0.5 \times 0.2 \times 2) = 8 \text{ cm}$$

(B) Theoretical dynamic corner displacements

From the curves ($e/r = 0.2$, and frequency ratio = 1.25) of Figs. 7(a), 9(a) and 4(a), the values of U , DAF, and ρ are obtained as: $U = 0.95$, DAF = 2.53, and $\rho = 0.77$.

$$U_\theta = \text{DAF}(e/r) = (2.53)(0.2) = 0.51.$$

$$U_{R1} = (0.51)(0.5 \times 2 - 0.2) = 0.41$$

$$U_{R2} = (0.51)(0.5 \times 2 + 0.2) = 0.61$$

Based on Eqs. (5) and (6),

$$U_{cm}^2 = U^2 + U_{R1}^2 + 2\rho U U_{R1}$$

$$= (0.95)(0.95) + (0.41)(0.41) + 2(0.77)(0.95)(0.41)$$

$$= 1.66$$

$$U_{cm} = 1.29$$

Based on the same process and Eq. (6), U_{ck} is calculated as

$$U_{ck} = 0.62$$

Therefore

$$U_{cm} = 10 \times 1.29 = 12.9 \text{ cm} > 12 \text{ cm}$$

$$U_{ck} = 10 \times 0.62 = 6.2 \text{ cm} < 8 \text{ cm}$$

and

$$u_x = 10 \times 0.95 = 9.5 \text{ cm}$$

$$u_\theta = 10 \times 0.51 = 5.1 \text{ cm}$$

Be aware that corner displacements calculated are larger than those calculated from the static analysis.

(C) Effective eccentricity

The effective eccentricity (e_f/r and e_r/r) could be back calculated from Eqs. (3) and (4),

$$U_{cm} = (1 + (e_f/r)(b/2r))$$

$$1.29 = (1 + (e_f/r))$$

$$e_f/r = 0.29$$

$$U_{ck} = (1 - (e_r/r)(b/2r))$$

$$0.62 = (1 - (e_r/r))$$

$$e_r/r = 0.38$$

It is also interesting to observe that effective eccentricities (e_f/r and e_r/r) are both larger than the mass eccentricity ($e/r = 0.2$) for this torsional stiff structure; however, only the $e_f/r = 0.29$ should be selected for design purpose.

Example 2. Consider the same structure as in Example (1) except that CM is at the center of geometry (SES).

(A) Static corner displacement

Corner displacement is calculated by applying equivalent static force on the CM, this is according to UBC but with the 5% b accidental eccentricity neglected here.

$$u_{cm} = 10 \times (1 + (e/r^2)(b/2 + e)) = 10(1 + 0.2(1 + 0.2)) = 12.4 \text{ cm}$$

$$u_{ck} = 10 \times (1 - (e/r^2)(b/2 - e)) = 10(1 - 0.2(1 - 0.2)) = 8.4 \text{ cm}$$

(B) Theoretical dynamic corner displacements

Follow the same process as above, from the curves ($e/r = 0.2$, and frequency ratio = 1.25) of Figs. 7(a), 9(a) and 4(a), the values of U , DAF, and ρ are obtained as: $U = 0.95$, DAF = 2.53, and $\rho = 0.77$.

$$U_{\theta} = \text{DAF}(e/r) = (2.53)(0.2) = 0.51$$

$$U_{R1} = 0.51$$

$$U_{R2} = 0.51$$

Based on Eqs. (5) and (6),

$$\begin{aligned} U_{cm}^2 &= U^2 + U_{R1}^2 + 2\rho U U_{R1} \\ &= (0.95)(0.95) + (0.51)(0.51) + 2(0.77)(0.95)(0.51) \\ &= 1.909 \end{aligned}$$

$$U_{cm} = 1.38$$

The same process as above can calculate U_{ck}

$$U_{ck} = 0.65$$

Therefore

$$\begin{aligned}u_{cm} &= 10 \times 1.38 = 13.8 \text{ cm} > 12.4 \text{ cm} \\u_{ck} &= 10 \times 0.65 = 6.5 \text{ cm} < 8.4 \text{ cm}\end{aligned}$$

and

$$\begin{aligned}u_x &= 10 \times 0.95 = 9.5 \text{ cm} \\u_\theta &= 10 \times 0.51 = 5.1 \text{ cm}\end{aligned}$$

(C) The effective eccentricity (e_f/r and e_r/r) could be back calculated

$$\begin{aligned}U_{cm} &= (1 + (e_f/r)(0.5b + e)/r) \\1.38 &= (1 + (e_f/r)(1 + e/r)) \\e_f/r &= 0.32 \\U_{ck} &= (1 - (e_r/r)(0.5b - e)/r) \\0.65 &= (1 - (e_r/r)(1 - e/r)) \\e_r/r &= 0.48\end{aligned}$$

It is interesting to observe that effective eccentricities (e_f/r and e_r/r) are both larger than those in Example 1.

The results from the example 1 and 2 (MES and SES but with the same eccentricity $e/r = 0.2$) demonstrates (1) the correlation based approach could calculate corner displacements for both cases; (2) the resulted effective eccentricities are different for two systems. ($e_f/r = 0.29$ for MES; $e_f/r = 0.32$ for SES).

5.4 Simulation results for different periods

As shown in Session 4, results for three structure periods are very similar to one another, therefore the average curves of ρ , U , and U_θ are presented for reference. These empirical curves or the theoretical curves in session 4 might be used for a quick estimation of the torsional effects. However, the characteristics of the earthquakes and white noise excitation could be further investigated to recommend curves better represent the design earthquakes. The authors are working on these issues currently.

5.5 Recommendation for torsional design

Static design of the asymmetrical structure is still accepted by most building codes. The applying of the lateral force on the structure will generate a maximum corner displacement (U_{cm}) proportional to eccentricity as in Fig. 1. However, according to the dynamic analysis, U_{cm} is a function of e_y/r , ω_θ/ω_x and ξ as indicated in Fig. 5(a). The discrepancy between the static analysis and dynamic analysis is the largest for structure with large eccentricity and/or $\omega_\theta/\omega_x < 1$. Therefore, for the design of earthquake resistant structures, dynamic analysis should be mandated for structure with large eccentricity or $\omega_\theta/\omega_x < 1$.

6. Conclusions

The correlation based approach demonstrates advantages over other approaches such as: theoretical solution available, not restricted by geometry models, best presenting the relation between torsional vibration and translational vibration and corner displacement, and a new way to obtain the theoretical dynamic corner displacement without dynamic analysis. However, the correlation coefficient, which should be the essential parameter for understanding the seismic response behavior of asymmetric building system, remains undiscovered for decades until this study.

Based on the theoretical and simulation results, we conclude the following:

1. Torsional vibration and translational vibration are strongly related, and this relationship is best represented by cross correlation factor ρ .
2. ρ is a function of three parameters: uncoupled frequency ratio, eccentricity, and damping ratio.
3. The uncoupled frequency is the dominating parameter to ρ . ρ is generally positive for $\omega_\theta/\omega_x > 1.0$, negative for $\omega_\theta/\omega_x < 1.0$, and close to zero for $\omega_\theta/\omega_x = 1.0$.
4. When eccentricity increases, ρ increases moderately only at small $\omega_\theta/\omega_x (< 1.0)$.
5. When damping increases, ρ also increases moderately only at small $\omega_\theta/\omega_x (< 1.0)$.
6. White noise approach appears satisfactory for the correlation study. It generate theoretical results match well with the results from earthquake simulation, and brings more insight with its formula for correlation coefficient.

As commonly recognized, proper application of the spectral method generally requires correct estimation of the torsional and translational periods of the structure. Likewise, the use of the proposed method to actual analysis/design structures require a proper consideration of the uncertainties involved in the estimation of the structure periods.

Note that although this paper emphasized the correlation concept and the theoretical solution for white noise earthquake input, it is possible to extend the methodology to general design earthquakes. The authors have been working on these subjects.

Acknowledgements

The authors would like to thank the National Science Council, Taiwan, Republic of China, for financially supporting this research under Contract No. NSC89-2211-E-011-061. All opinions expressed herein are solely those of the writers and do not necessarily reflect the view of the sponsors.

References

- Chandler, A.M. and Hutchinson, G.L. (1988), "Evaluation of the secondary torsional design provisions of earthquake building codes", *Proc. Inst. Civ. Engrs. Part 2*, **85**, 587-607.
- Der Kiureghian, A. (1981), "A response spectrum method for random vibration analysis of MDOF systems", *Earthq. Eng. and Struct. Dyn.*, **9**, 419-435.
- Jeng, V. and Kasai, K. (1996), "Spectral relative motion of two structures due to seismic travel waves", *J. Struct.*

- Eng.*, ASCE, **122**(10), 1128-1135.
- Kan, C.L. and Chopra, A.K. (1976), "Coupled lateral torsional response of buildings to ground shaking", Report No. UCB/EERC-76/13, Earthquake Engineering Research Center, University of California, Berkeley.
- Kan, C.L. and Chopra, A.K. (1979), "Linear and nonlinear earthquake responses of simple torsionally coupled systems", Report No. UCB/EERC-79/03, Earthquake Engineering Research Center, University of California, Berkeley.
- Pan, T.C. and Kelly, J.M. (1983), "Seismic response of torsionally coupled base isolated structures", *Earthq. Eng. and Struct. Dyn.*, **11**, 749-770.
- Rosenblueth, E. and Meli, R. (1986), "The 1985 earthquake: causes and effects in Mexico City", *Concrete int.*, **8**(5), 23-34.
- Rutenberg, A. and Pekau, O.A. (1987), "Seismic code provisions for asymmetric structures: a re-evaluation", *Eng. Struct.*, **9**, 255-264.
- Tso, W.K. and Dempsey, K.M. (1980), "Seismic torsional provisions for dynamic eccentricity," *Earthq. Eng. and Struct. Dyn.*, **8**, 275-285
- Uniform Building Code. (1997), *Int. Conf. of Building Officials*, Whittier, California.

Notation

The following symbols are used in this paper:

b	: dimension of structure perpendicular to the direction of earthquake input;
CM	: center of mass;
CK	: center of stiffness;
$[C]$: damping matrix;
DAF	: dynamic amplification factor for torsional displacement;
e	: eccentricity;
e_f	: effective eccentricity at CM side;
e_r	: effective eccentricity at CK side;
e_y	: eccentricity in Y-direction;
f_{CN}	: function;
G_0	: power spectral density of the white noise excitation;
K_x	: assembled stiffness in X-direction;
K_θ	: assembled torsional stiffness about Z-axis;
K_ρ	: peak factor;
L_i	: modal participation factor in the i^{th} mode;
m	: assembled lateral mass and torsional mass at CM;
m_θ	: assembled torsional mass at CM;
$q_i(t)$: spectral response of i^{th} mode;
$u_0(t)$: translational displacement of uncoupled system ($e = 0$);
$u_{ck}(t)$: corner displacement at center of stiffness side;
$u_{cm}(t)$: corner displacement at center of mass side;
$u_{R1}(t)$: contribution of $\theta(t)$ to the corner displacement at CM side;
$u_{R2}(t)$: contribution of $\theta(t)$ to the corner displacement at CK side;
$u_x(t)$: translational displacement;
$u_\theta(t)$: torsional displacement;
q_i	: $\max q_i(t) $;
T	: translational period ($2\pi/\omega_x$);
u_0	: $\max u_0(t) $;
u_{ck}	: $\max u_{ck}(t) $;
u_{cm}	: $\max u_{cm}(t) $;
u_{R1}	: $\max u_{R1}(t) $;
u_{R2}	: $\max u_{R2}(t) $;

u_x	: $\max u_x(t) $;
u_θ	: $\max u_\theta(t) $;
$\ddot{u}_{gx}(t)$: ground acceleration in the X-direction;
U	: normalized peak displacement of u_x ;
U_{ck}	: normalized peak corner displacement of u_{ck} ;
U_{cn}	: normalized peak corner displacement of u_{cn} ;
U_θ	: normalized peak torsional displacement of u_θ ;
$y_i(t)$: modal responses for i^{th} mode;
y_i	: $\max y_i(t) $;
r	: radius of gyration of the stiffness;
r_{12}	: ω_1/ω_2 ;
r_q	: q_1/q_2 ;
$\{r\}$: the influence coefficient vector;
$\theta(t)$: angular displacement about Z-axis;
θ	: $\max \theta(t) $;
ξ_i	: the modal damping ratio for i^{th} mode;
ρ	: the cross correlation coefficient between u_x and u_θ ;
ρ_{12}	: the correlation between mode 1 and mode 2;
ϕ^i	: modal shape for i^{th} mode;
ω_i	: modal natural frequency for i^{th} mode;
ω_x	: the uncoupled translational frequency;
ω_θ	: the uncoupled torsional frequency; and
Ω	: the uncoupled frequency ratio (ω_θ/ω_x);